Deterministic and Random Targets in Frequency Diverse Imaging

J.W. Bredow, A.K. Fung, R. Porco, G. Hartman

University of Texas at Arlington - Box 19016 Arlington, TX 76019 USA

ABSTRACT

This research is concerned with furthering the understanding and interpretation of microwave diversity images in terms of scattering phenomena at the object being imaged. Two imaging methods are used: (1) multistatic, where the illumination polarization and direction are constant with respect to the object while the receiver is varied over azimuth; and (2) bistatic or monostatic, where the object is rotated with respect to fixed illuminating and receiving antennas. Note that the former is considered to be of importance because image intensities can be well related to the target's induced currents (see section I), whereas the latter is a consequence of the usual configuration for airborne and spaceborne radars. In this paper we consider the development of a system to perform the first method of imaging, and study images obtained of simple deterministic targets using both methods. Only qualitative assessments of the results are made in this report. However, future efforts will focus on extensively contrasting images obtained using both methods. Note that we expect this research to help us better understand imaging of random conducting surfaces in terms of the physical characteristics of isolated patches of the surface.

INTRODUCTION

Previously we performed scattering measurements on statistically known randomly rough conducting surfaces, and processed the data to obtain both scattering coefficients and inverse SAR (ISAR) images, [Nance et al., 1988] and [Nance et al., 1990]. The scattering coefficient data has been very useful for assessing the performance of various surface scattering models, but the images have been difficult to interpret. For this reason we have embarked on a systematic investigation to study the relationships between image intensity and electromagnetic interaction (in terms of induced sources) for various conducting objects, beginning with simple ones.

In microwave diversity imaging of metallic objects a commonly used expression for retrieving images from a set of scattering measurements obtained over frequency and space has the form [Li et al, 1989]:

$$\mathbf{E}_s(\overline{\mathbf{p}}) = \int_{sill} \overline{\gamma}'(\mathbf{bar}', \overline{\mathbf{p}})\, e^{j\overline{p}\cdot\overline{r}'}\, ds'$$

where
the object scattering function

$$\overline{\gamma}'(\overline{\mathbf{r}}', \overline{\mathbf{p}}) = \begin{cases} \hat{\mathbf{n}}(\overline{\mathbf{r}}') \times \mathbf{H}_i^\circ - [(\hat{\mathbf{n}}(\overline{\mathbf{r}}') \times \mathbf{H}_i^\circ) \cdot \hat{\mathbf{I}}_\mathbf{r}]\, \hat{\mathbf{I}}_\mathbf{r} \\ \text{for all } \overline{\mathbf{r}}' \text{ on } S_{ill} \\ 0, \text{ elsewhere} \end{cases}$$

$\mathbf{E}'_s(\overline{\mathbf{p}})$ represents the scattered fields
$\overline{\mathbf{p}} = k(\hat{\mathbf{I}}_\mathbf{r} - \hat{\mathbf{I}}_\mathbf{t})$
S_{ill} is the illuminated surface region
$\mathbf{H}_i^\circ$ is the incident magnetic field at the reference point
$\hat{\mathbf{n}}(\overline{\mathbf{r}}')$ is the unit normal vector at $\overline{\mathbf{r}}'$
$\hat{\mathbf{I}}_r$ is the unit vector in the direction of the receiver
$\hat{\mathbf{I}}_t$ is the unit vector in the direction of the transmitter

Although this inversion expression is strictly valid only for a limited class of targets, it is commonly used to generate images of a wide variety of targets because of its simplicity. Note that the object function and the scattered fields are related by a Fourier Transform-type of relationship, i.e., Fourier and Fast Fourier techniques can be used to obtain one from the other.

For the above expression it should be noted that for conducting targets the $\hat{\mathbf{n}}(\overline{\mathbf{r}}') \times \mathbf{H}_i^\circ$ term in the object function relates to sources on the target; this is a result of the boundary condition $\mathbf{J} = \hat{\mathbf{n}}(\overline{\mathbf{r}}') \times \mathbf{H}_i^\circ$. One implication of this is that as imaging measurements are performed in the usual monostatic or bistatic fashion (i.e., the target is rotated and the antennas remain stationary), the set of source currents on the target varies as scattering measurements are obtained. For the purpose of relating image intensities to sources on

the object a better scheme is to maintain illumination from a constant direction as the receiver samples the scattered fields from various directions.
Below are reported preliminary results for a number of aspects pertaining to the stated problem. We consider the effects of sampling aperture size, polarization, creeping waves, and compare the cases of bistatic or monostatic imaging (i.e., varying illumination) and constant illumination.

1. FACILITY DEVELOPMENT AND MODIFICATIONS

1.1 Monostatic and bistatic (varying illumination)

The microwave anechoic measurement facility at the University of Texas at Arlington Wave Scattering Research Center was designed to facilitate bistatic measurements. An array of 27 receive antennas over a quarter-sphere section at constant radius from the pedestal and three transmit antennas permit 81 bistatic angle measurements of a stationary target. Hence, monostatic and bistatic data for images can be obtained using the facility as it was originally designed, i.e., by performing scattering measurements as the target is rotated.

1.2 Constant illumination

One significant drawback in the design of the UTA anechoic chamber is that it did not permit measurements for the case where only the receive antenna is moved. To facilitate imaging measurements with constant illumination direction we fabricated an antenna mount that rotates with the positioner pedestal, using lexan plastic components (see drawing in Fig. 1). This allows us to maintain a constant spatial relationship between the transmit antenna and target, and scanning of the receive antenna occurs as the pedestal is rotated. To ensure phase coherency it was necessary to prevent motion in the cable that feeds the transmit antenna; this was accomplished by feeding the arm-mounted antenna through a rotary joint at the base of the pedestal.
In addition to hardware modifications, some software modifications have been necessary. The routines developed previously at UTA for obtaining images from scattering measurements [Dolaty, 1989] are restricted to the more conventional cases of bistatic and monostatic imaging. This is due to the method used to interpolate the scattering data points onto a uniformly spaced grid, i.e., so that standard FFT routines can be used to perform the inversion.

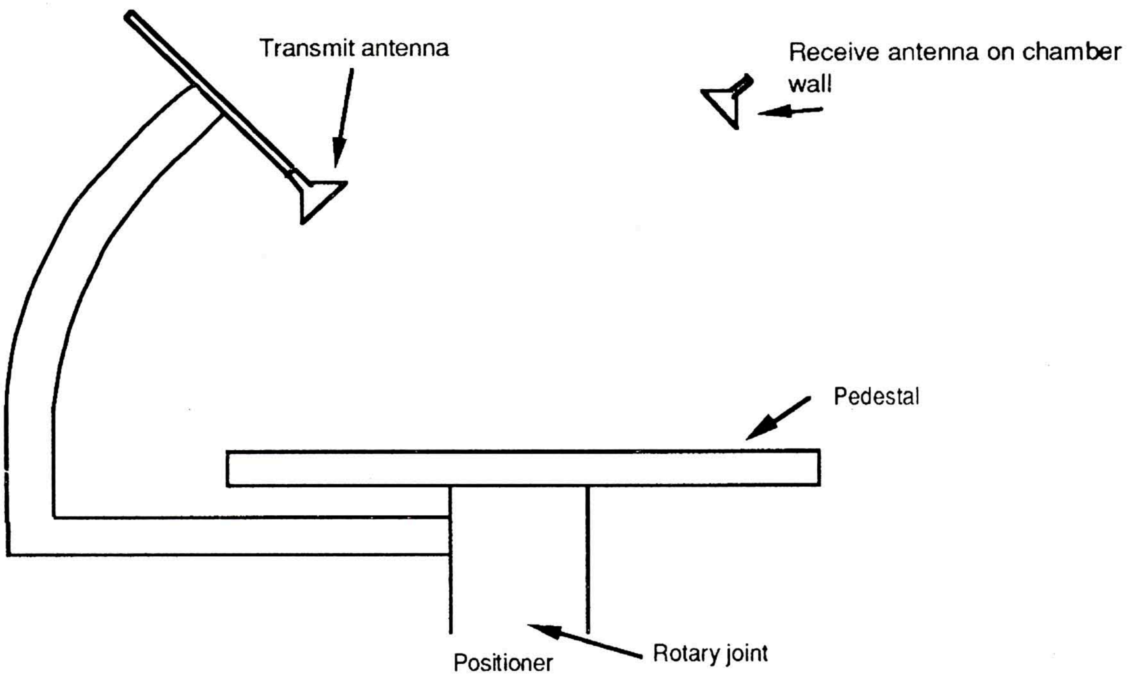

Fig. 1 - Setup for measurements using constant illumination.

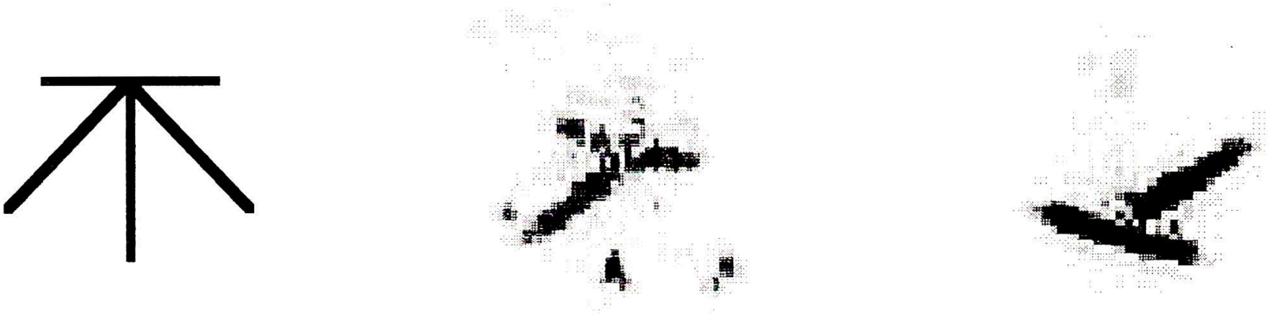

a) geometric arrangement

b) image over azimuth -45° to $+45^\circ$ for 45° bistatic angle

c) image over azimuth -45° to $+45^\circ$ for 45° bistatic angle after rotating target

Fig. 2 - Arrangement of four cylinders with two orientations (Diameter = 2.5 cm, Length = 20 cm).

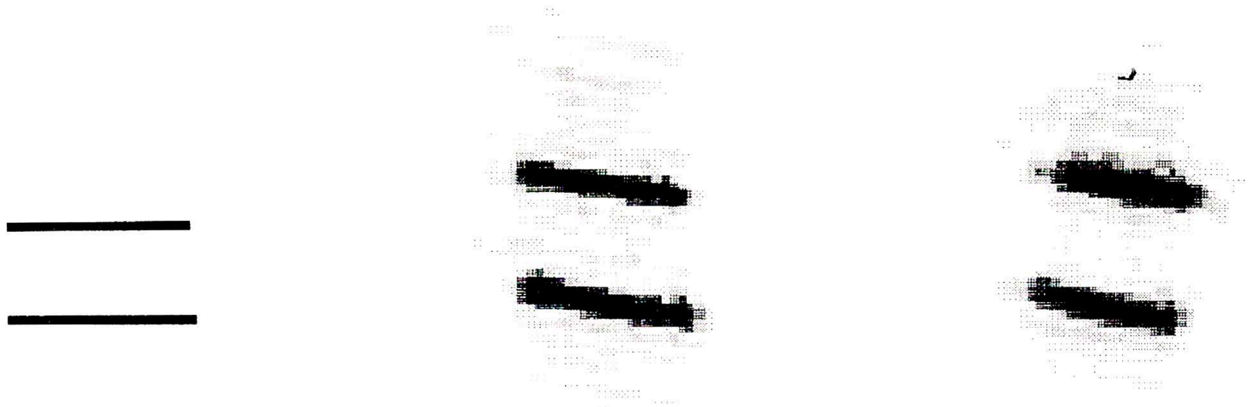

a) geometric arrangement

b) VV-polarization image for 45° bistatic angle

c) HH-polarization image for 45° bistatic angle

Fig. 3 - Arrangement of two parallel cylinders at VV and HH polarizations (Diameter = 2.5 cm, Length = 20 cm, Spacing = 16 cm).

2. MEASUREMENT RESULTS AND DISCUSSION

It should be noted that all images reported here were obtained using a frequency sweep of 4-12 GHz, elevation angles of about 45°, and angular measurement aperture of 90°.

Consider the effect of target orientation: Figure 2a shows an arrangement of four cylinders and Fig. 2b shows the microwave image for a 45° bistatic angle between transmit and receive antennas. For Fig. 2c the target was rotated and imaging was performed over the same aperture as was used to obtain Fig. 2b. Note in Fig. 2b that two of the cylinders are clearly seen, whereas the other two are apparent only as a result of scattering and diffraction at the ends of the cylinders. For the other orientation (Fig. 2c), two of the cylinders are not seen at all. Clearly a wider imaging aperture, i.e., greater than the 90° aperture used here, would have yielded more complete images. This result alludes to the importance of having information about target symmetries before selecting the angular size of the measurement aperture.

Consider the effect of polarization: Figure 3 shows an arrangement of two parallel cylinders and the resulting images for VV and HH polarizations with 45° bistatic angle. Note that nearly identical images were obtained in both cases. Two possible reasons for this are: (1) these cylinders are not thin in terms of wavelengths; and (2) the elevation angle of the antennas is sufficiently large that considerable coupling would occur even for HH polarization. Certainly this effect needs to be studied functionally with respect to cylinder dimensions and elevation angle before definitive statements can be made concerning polarization.

Figure 4 illustrates the effect of creeping waves on images: here an arrangement of four loops of varying size and lying in a horizontal plane is imaged using horizontal polarization with 45° bistatic angle. Note that the sides of the individual loops are not discernible, although scattered fields from each of the loops are apparent. It seems that creeping waves were responsible for blurring of the actual loops (indicated by arrows in the figure) and ghosting that causes the image to appear as though much larger loops are present. However, larger angular measurement apertures and further measurements of loops larger than the largest loop considered here, i.e., 6-cm diameter, are needed to further define the effects.

Note that Fig. 5b is one of our earliest images for the case of constant illumination. The strong returns indicated by the arrows are due to the spheres illustrated in Fig. 5a. Note that some noise is apparent in the image; this is a

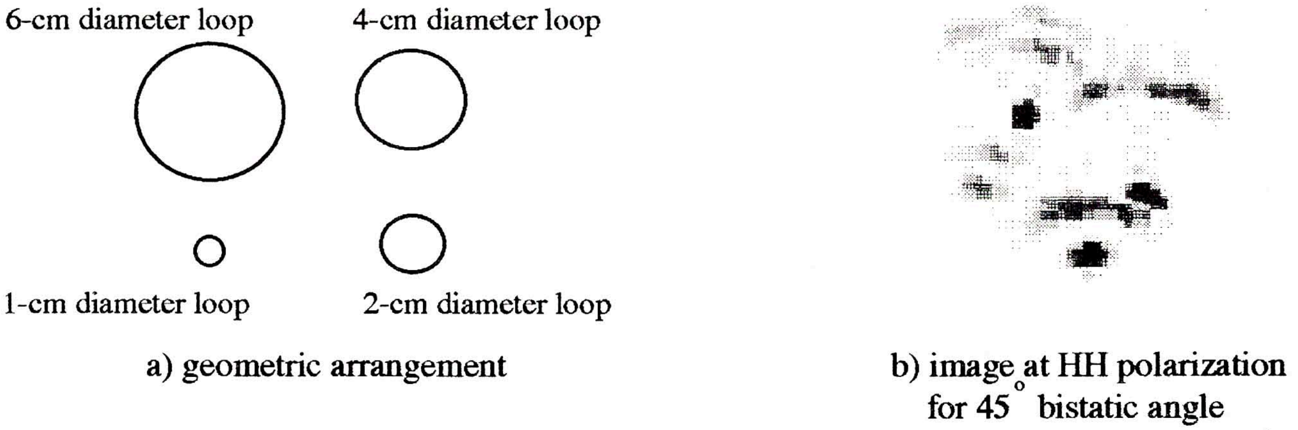

Fig. 4 - Four loops of varying size (Spacing = 14 cm, wire diameter = 3 mm).

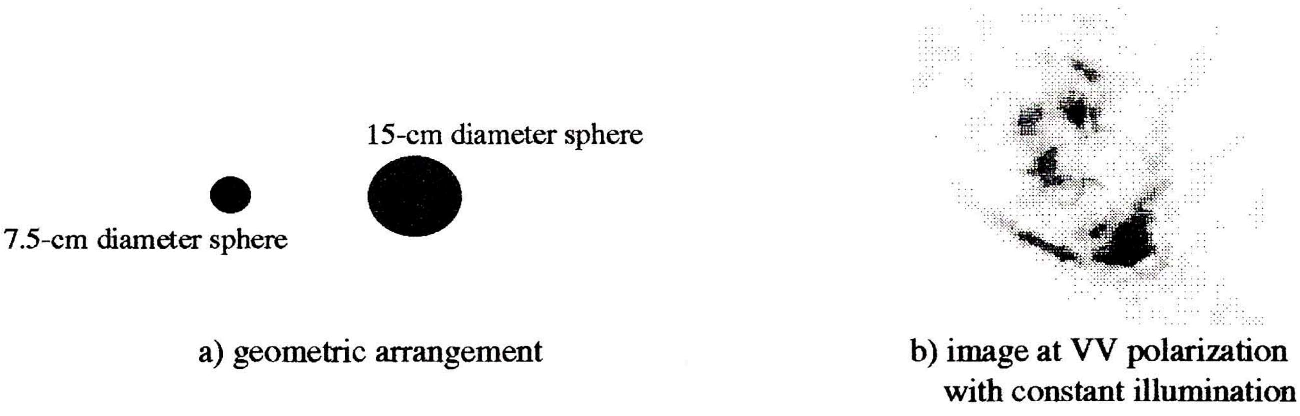

Fig. 5 - Two spheres of varying size (Spacing = 30 cm).

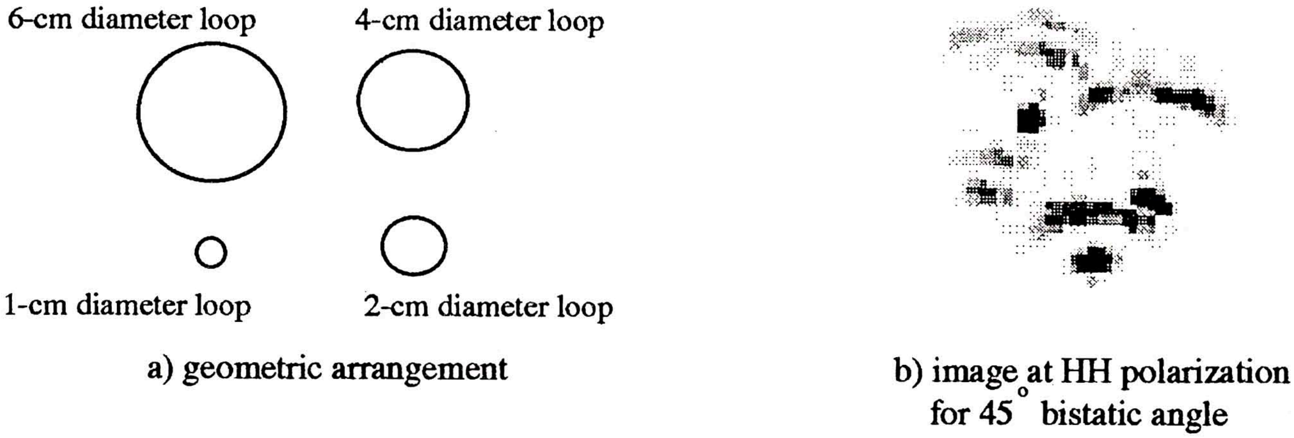

Fig. 6 - Comparison of two imaging techniques for two parallel cylinders.

result of motion in the moving antenna mount, i.e., that connected to the pedestal. Other than the noise the image is nearly identical to what we would expect for the monostatic and near-monostatic imaging cases.

Figure 6 shows a comparison between bistatic imaging (45° bistatic angle) and constant -illumination imaging for the case of two parallel cylinders. In this case the resulting images are dramatically different. At this point we are unable to pinpoint the differences between the two images in terms of scattering theory. However, it should be reiterated that the constant-illumination image is obtained by inverting a spatial scattering pattern for a given set of source currents (analogous to an antenna problem), whereas the bistatic image is obtained by inverting data points from a set of spatial scattering patterns. Because of the latter, we believe that studies of constant-illumination imaging can lead to a better understanding of the more conventional bistatic and monostatic imaging cases.

3. SUMMARY AND FURTHER WORK

This report has considered, in a rather cursory fashion, a number of aspects pertinent to relating intensity in frequency diverse microwave images to scattering phenomena at the targets being imaged. We have considered the effects of object orientation (or angular measurement aperture), polarization, ringing or creeping waves, and imaging method. All of these are important effects. However, we would like to emphasize the significance of performing constant-illumination imaging measurements as a means for better understanding imaging in terms of induced sources at the target.

In this report we have indicated the theoretical basis for emphasizing constant-illumination measurements, the development of a facility for performing such measurements, and preliminary results using this facility.

In the future we expect to continue to investigate all of the problems stated above. However, we intend to make extensive comparisons between conventional bistatic or monostatic imaging and constant-illumination imaging to: (1) obtain a better understanding of how image intensity relates to induced sources on the target; and (2) to better understand imaging for the conventional imaging geometries. Note that we expect this research to lead to a more complete knowledge of imaging of random conducting surfaces in terms of scattering from individual roughness elements of the surface.

BIBLIOGRAPHY

Dolaty, M., Inverse synthetic aperture radar imaging techniques, M.S. thesis, University of Texas at Arlington, 1989.

Li, H.J., N.H. Farhat, Y. Shen and C.L. Werner, "Image understanding and interpretation in microwave diversity imaging," IEEE Transactions on Antennas and Propagation, v. 37, no. 8, pp. 1048-1057, 1989.

Nance, C.E., A.J. Blanchard, and M. Chen, "Polarimetric microwave scattering from known randomly rough surfaces," Proc. IGARSS '88 Symposium, Edinburgh, Scotland, 1988.

Nance, C.E., A.K. Fung, and J.W. Bredow, "Comparison of integral equation predictions and experimental backscatter measurements from random conducting rough surfaces," Proc. IGARSS '90 Symposium, College Park, MD, 1990.